

Figure 5. 2 m air temperature differences (in $^{\circ}\text{C}$) between the GCM driven RCAO simulations during the control period (December 1968 to November 1998) and the hindcast simulation using RCA3 forced with ERA40. From left to right differences for the four seasons (DJF, MAM, JJA and SON) and for the annual mean are shown. The rows correspond to the RCAO simulation forced with HadCM3-A1B (first row)), ECHAM5-A1B_3 (second row), ECHAM5-A1B_1 (third row) and ECHAM5-A2 (fourth row).

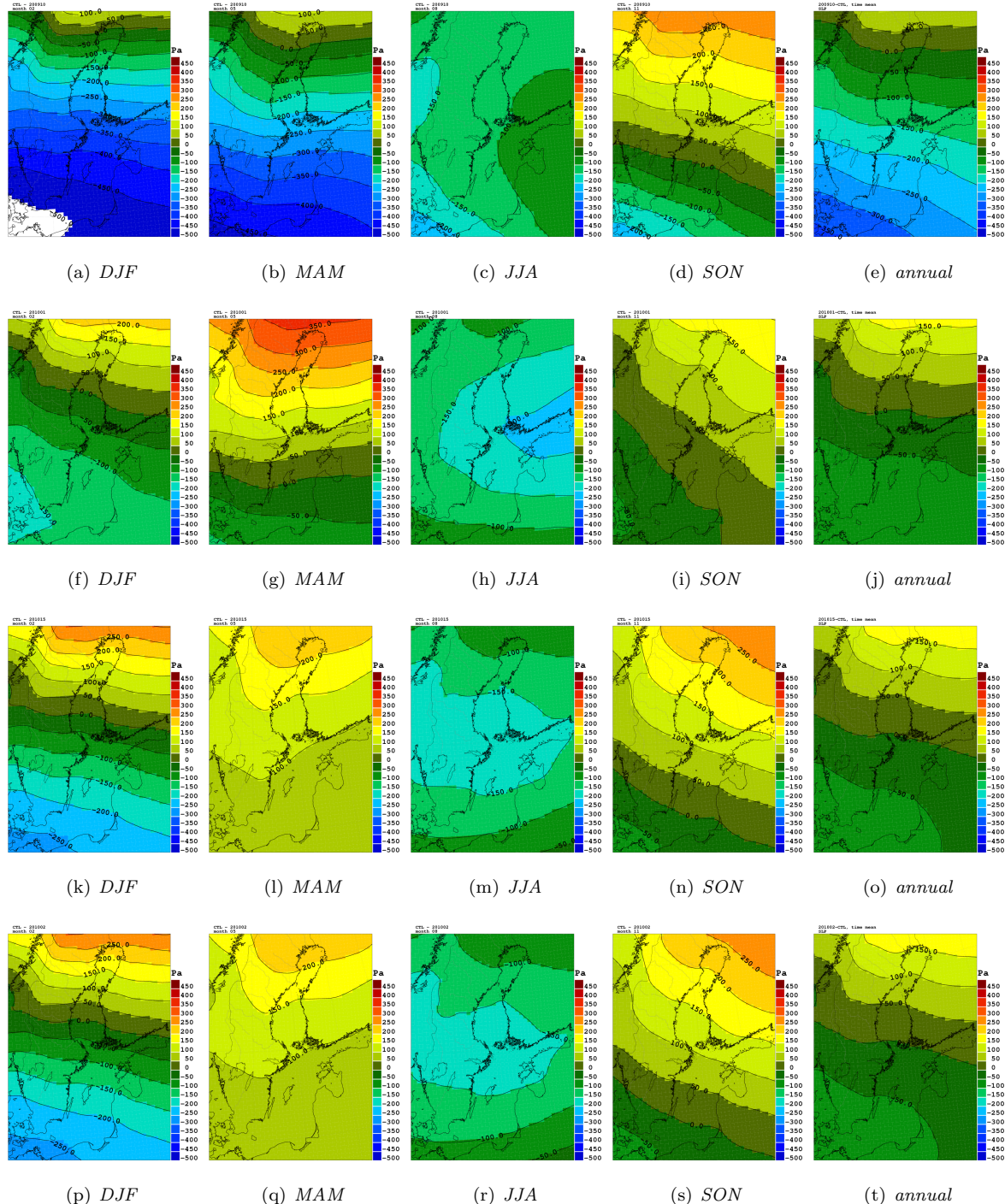


Figure 6. Same as Figure 5 but for sea level pressure (in Pa).

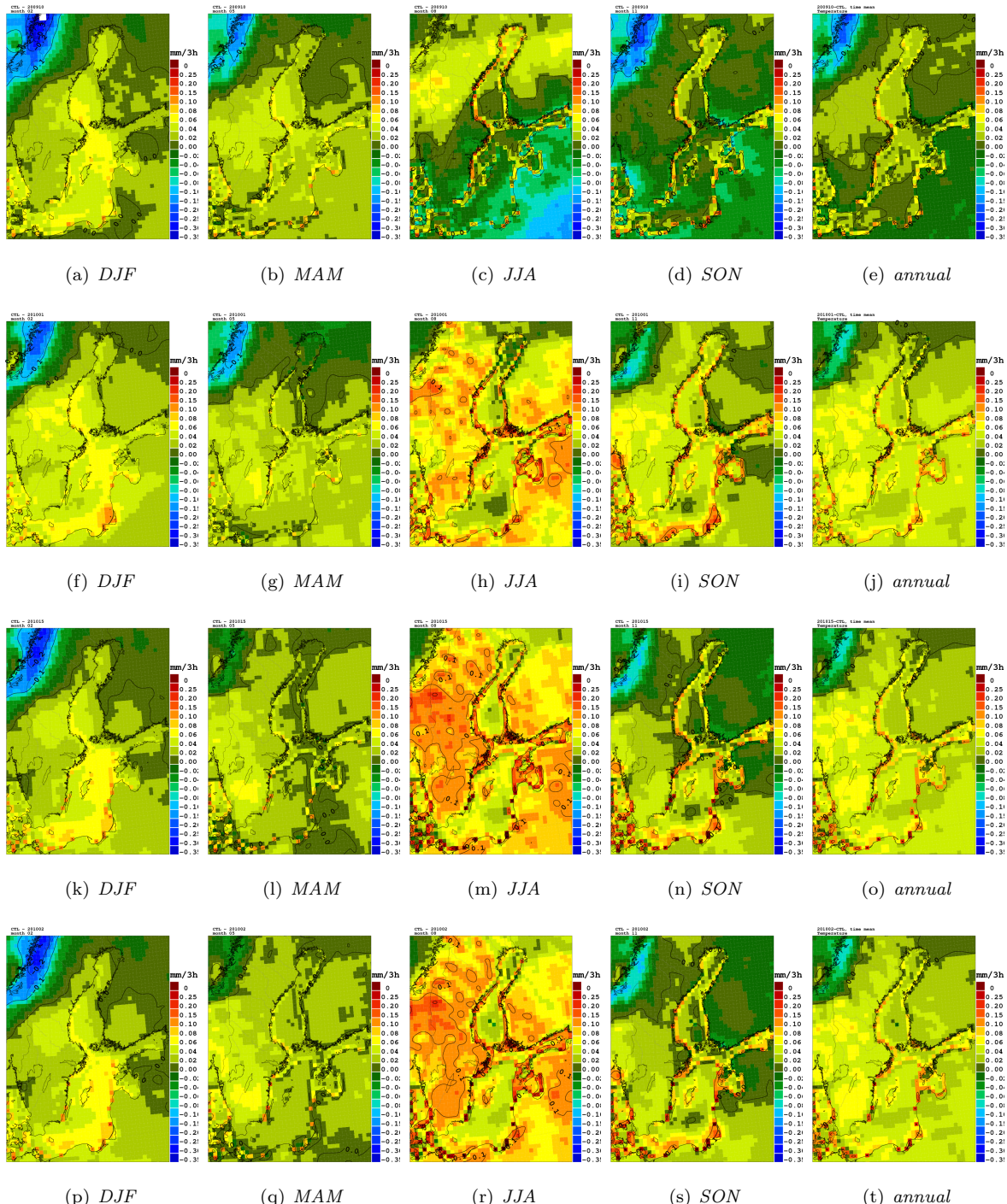


Figure 7. Same as Figure 5 but for precipitation (in mm/3h).

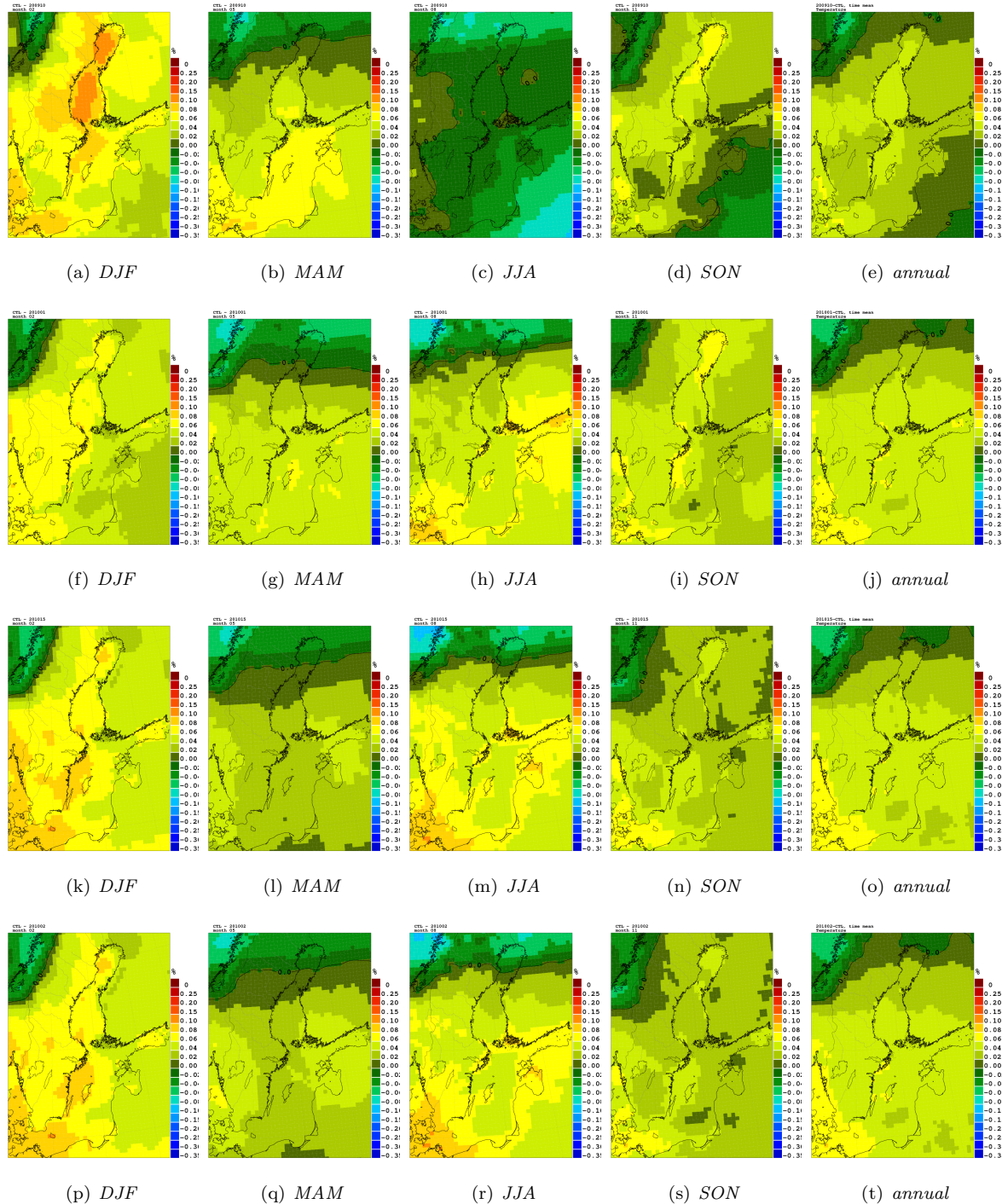


Figure 8. Same as Figure 5 but for cloud cover.

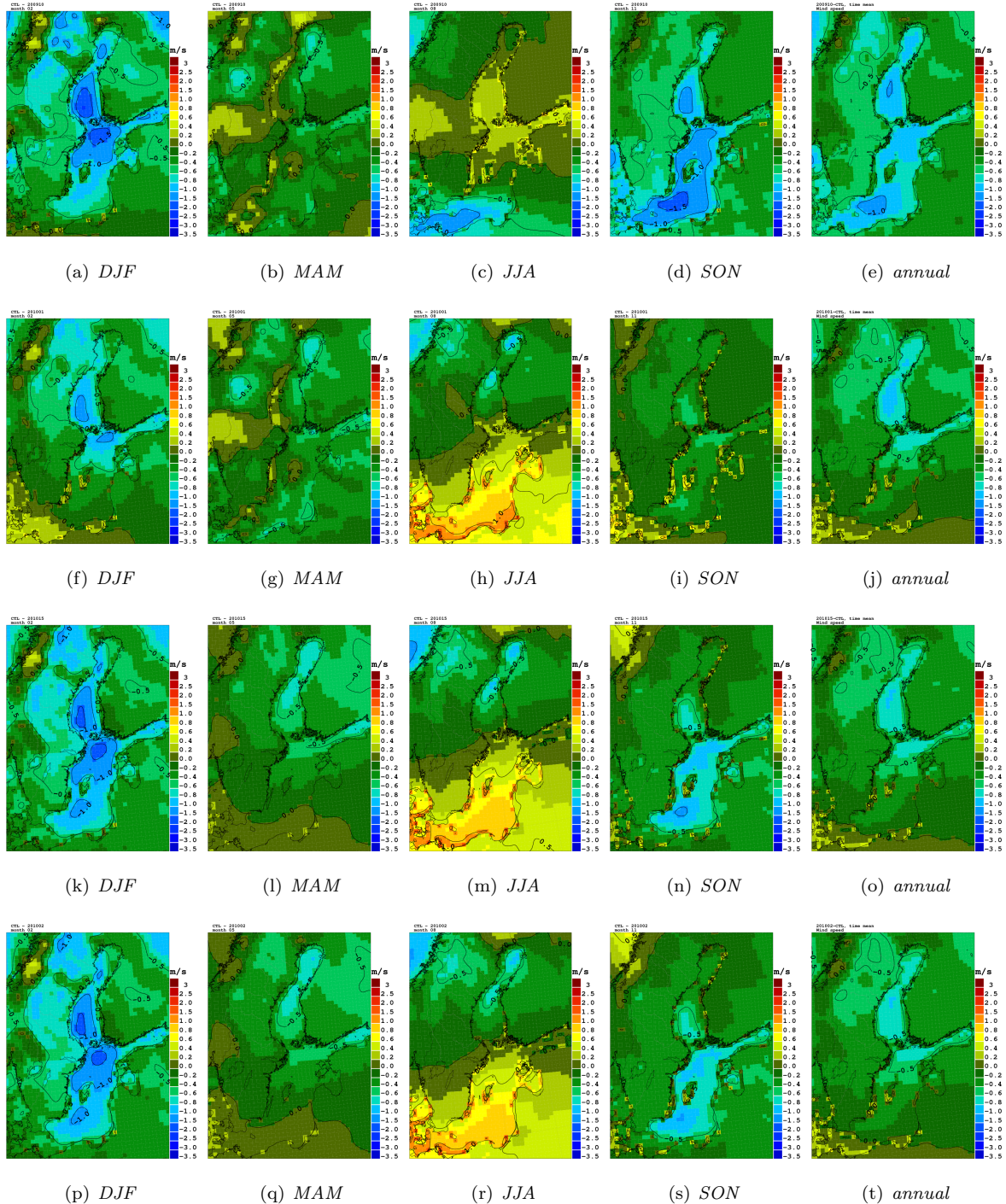


Figure 9. Same as Figure 5 but for the mean 10 m wind speed (in m/s).

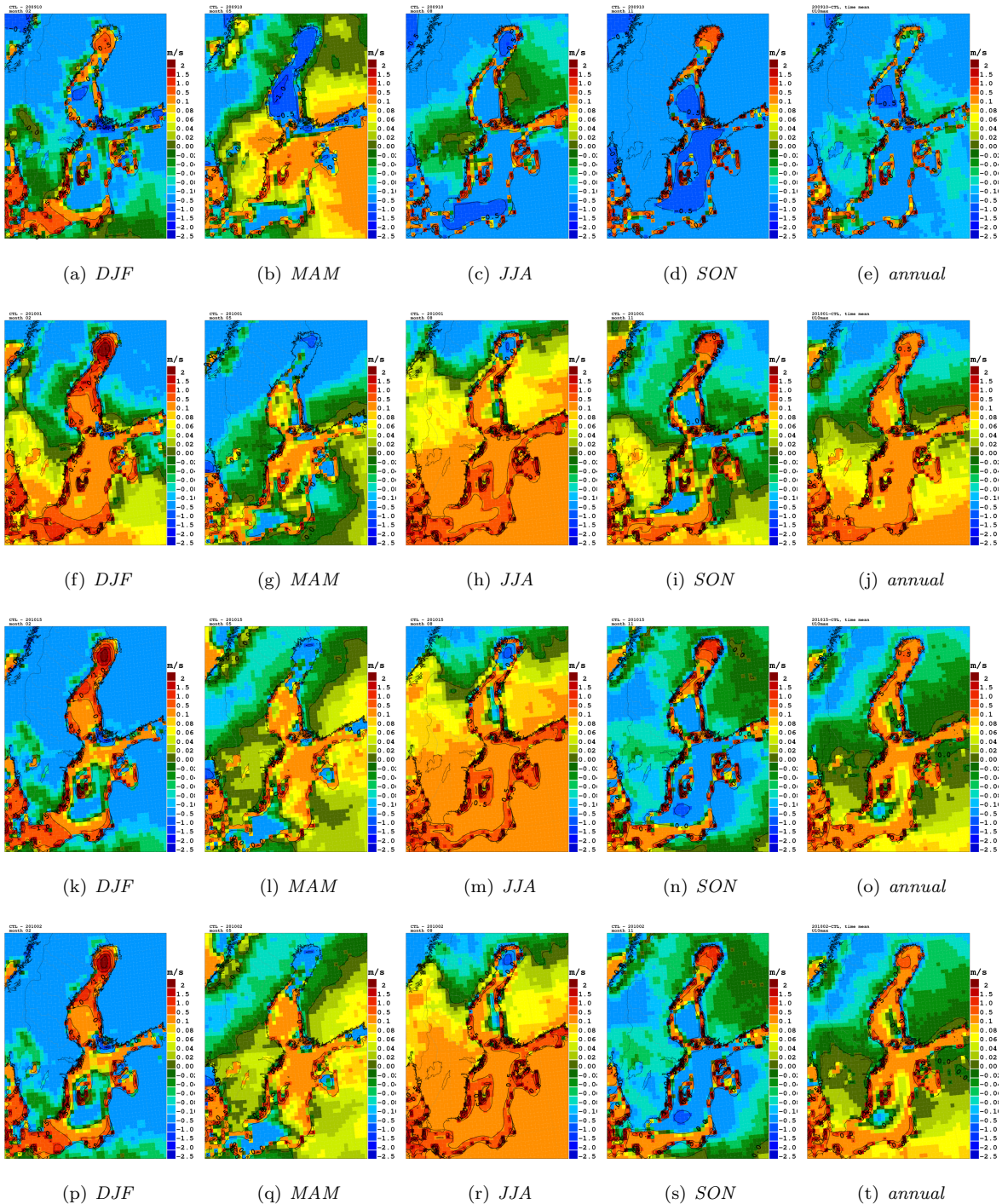


Figure 10. Same as Figure 5 but for the maximum 10 m wind speed (in m/s).

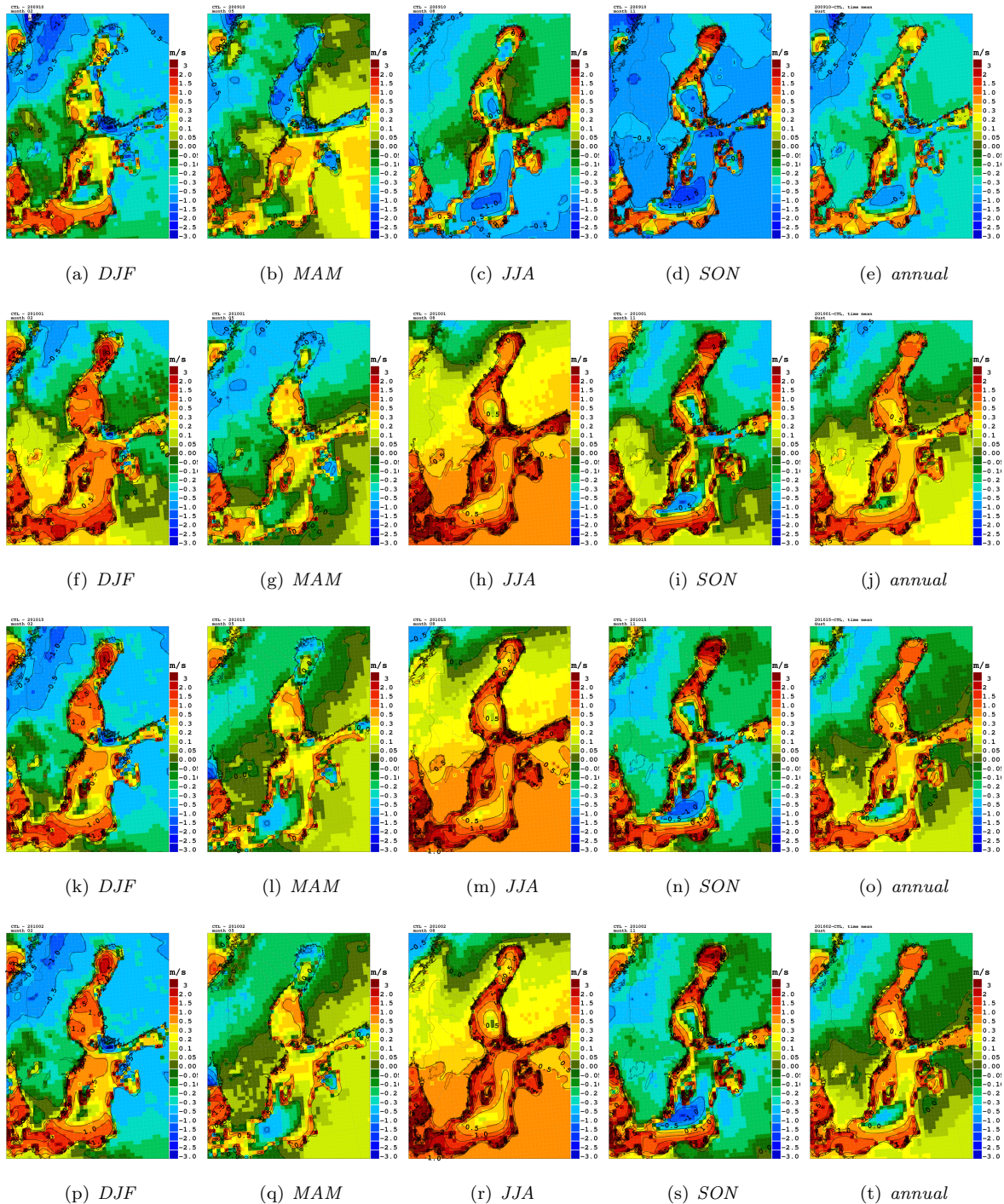


Figure 11. Same as Figure 5 but for the maximum estimated gust wind (in m/s).

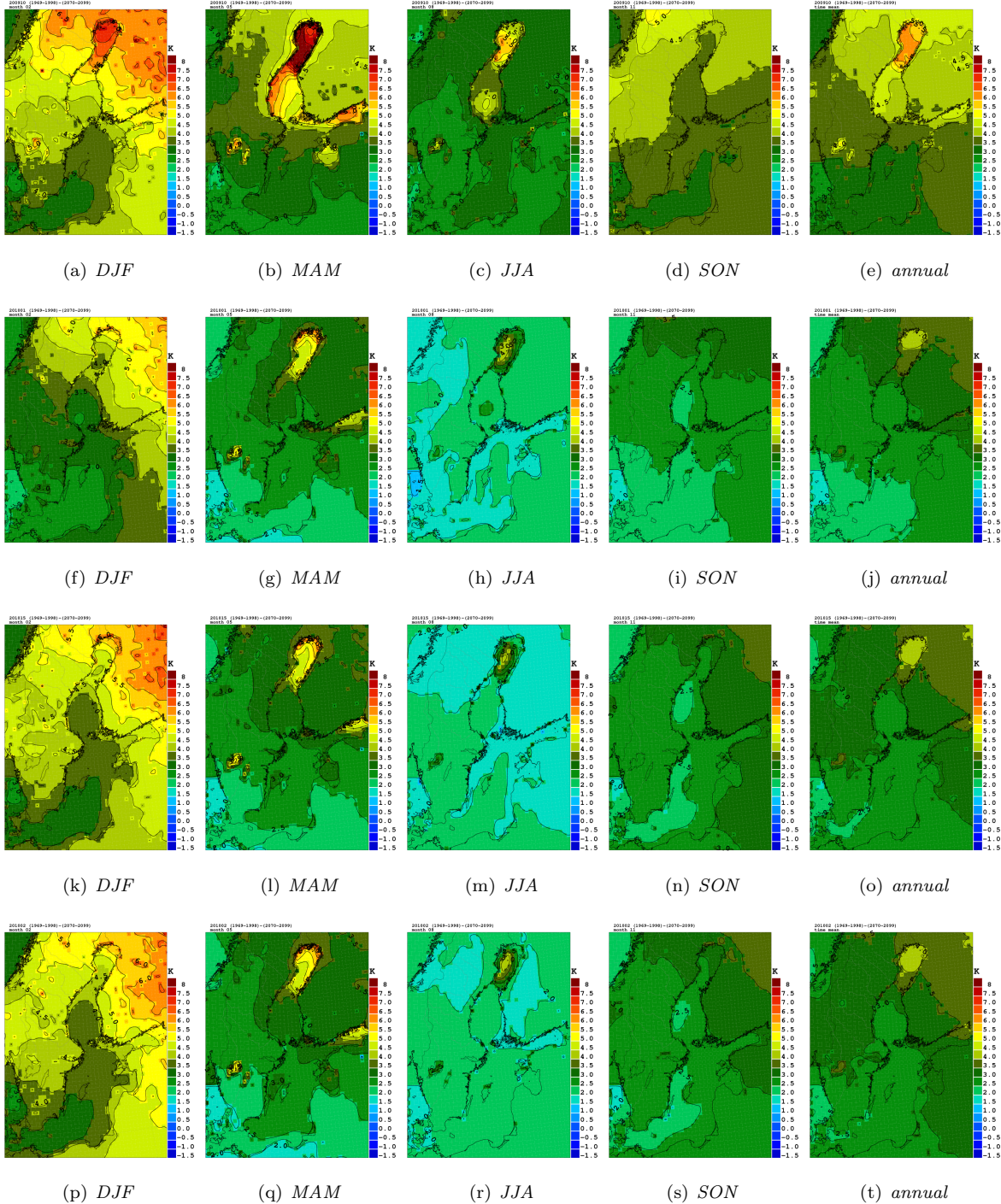


Figure 12. 2 m air temperature differences (in $^{\circ}\text{C}$) between the projected changes at the end of the 21st century (November 2069 until December 2099) and the control period (December 1969 until November 1998). From left to right differences for the four seasons (DJF, MAM, JJA and SON) and for the annual mean are shown. The rows correspond to the RCAO simulations forced with HadCM3-A1B (first row), ECHAM5-A1B_3 (second row), ECHAM5-A1B_1 (third row) and ECHAM5-A2 (fourth row).

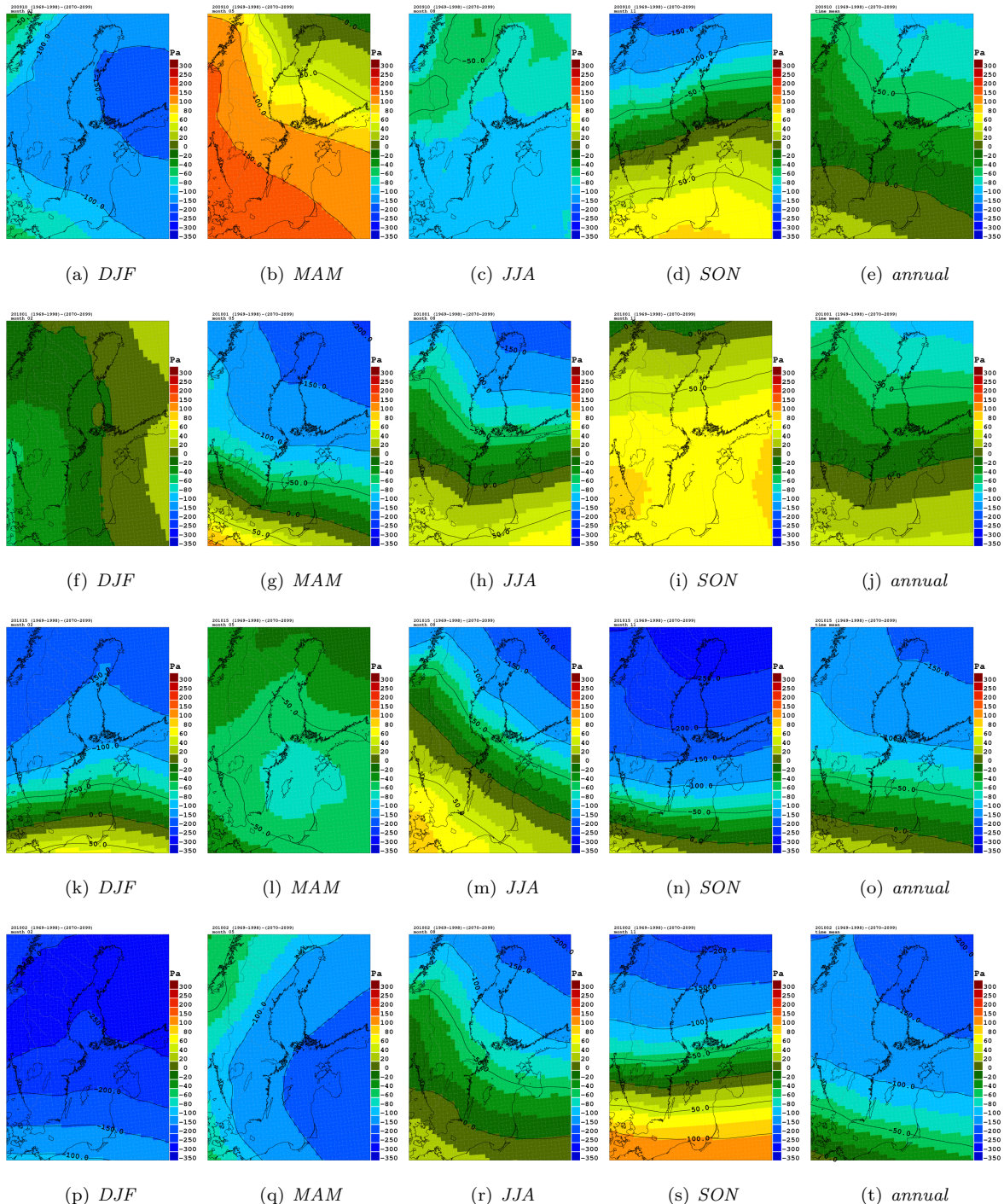


Figure 13. Same as Figure 12 but for sea level pressure (in Pa).

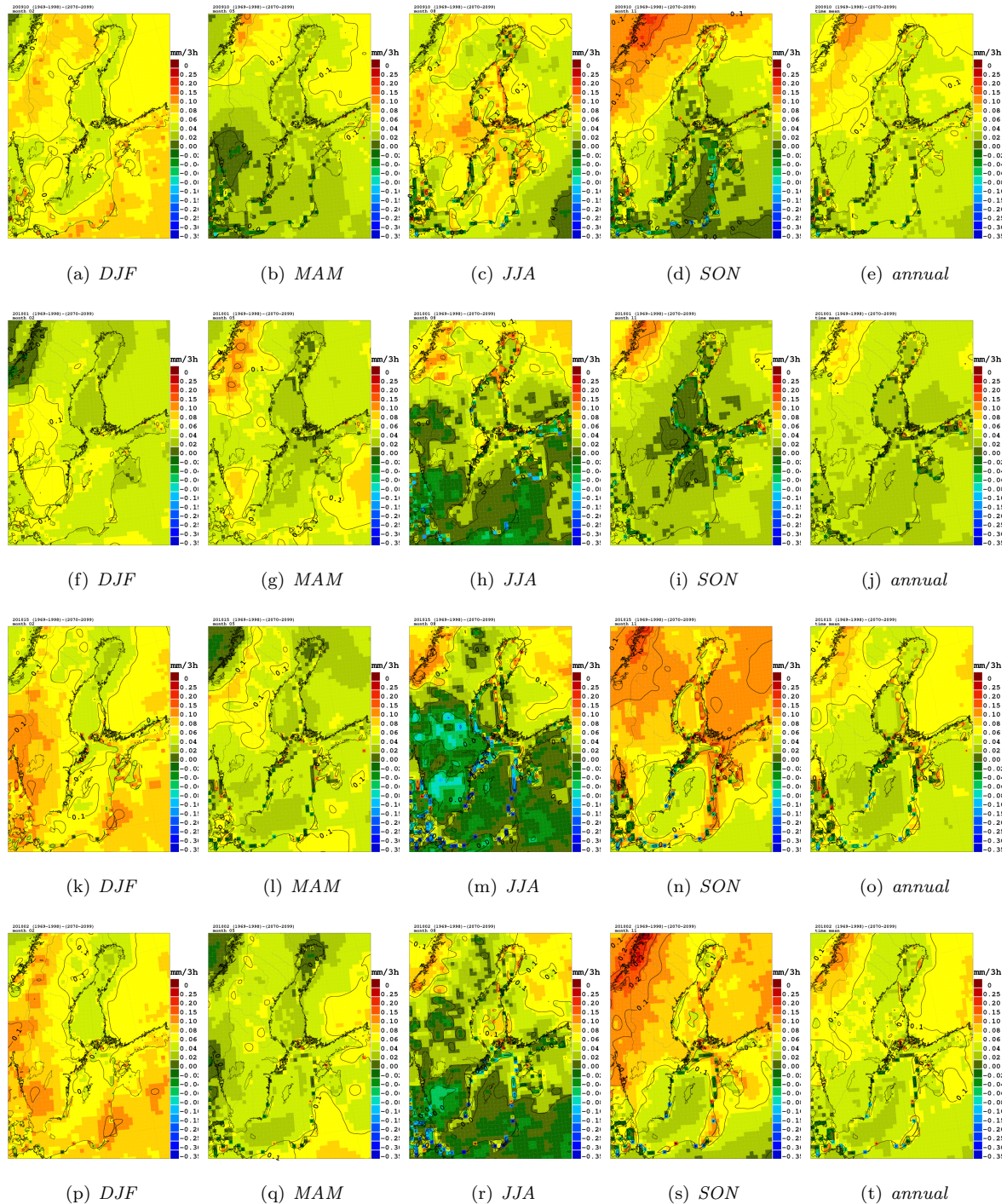


Figure 14. Same as Figure 12 but for precipitation (in mm/3h).

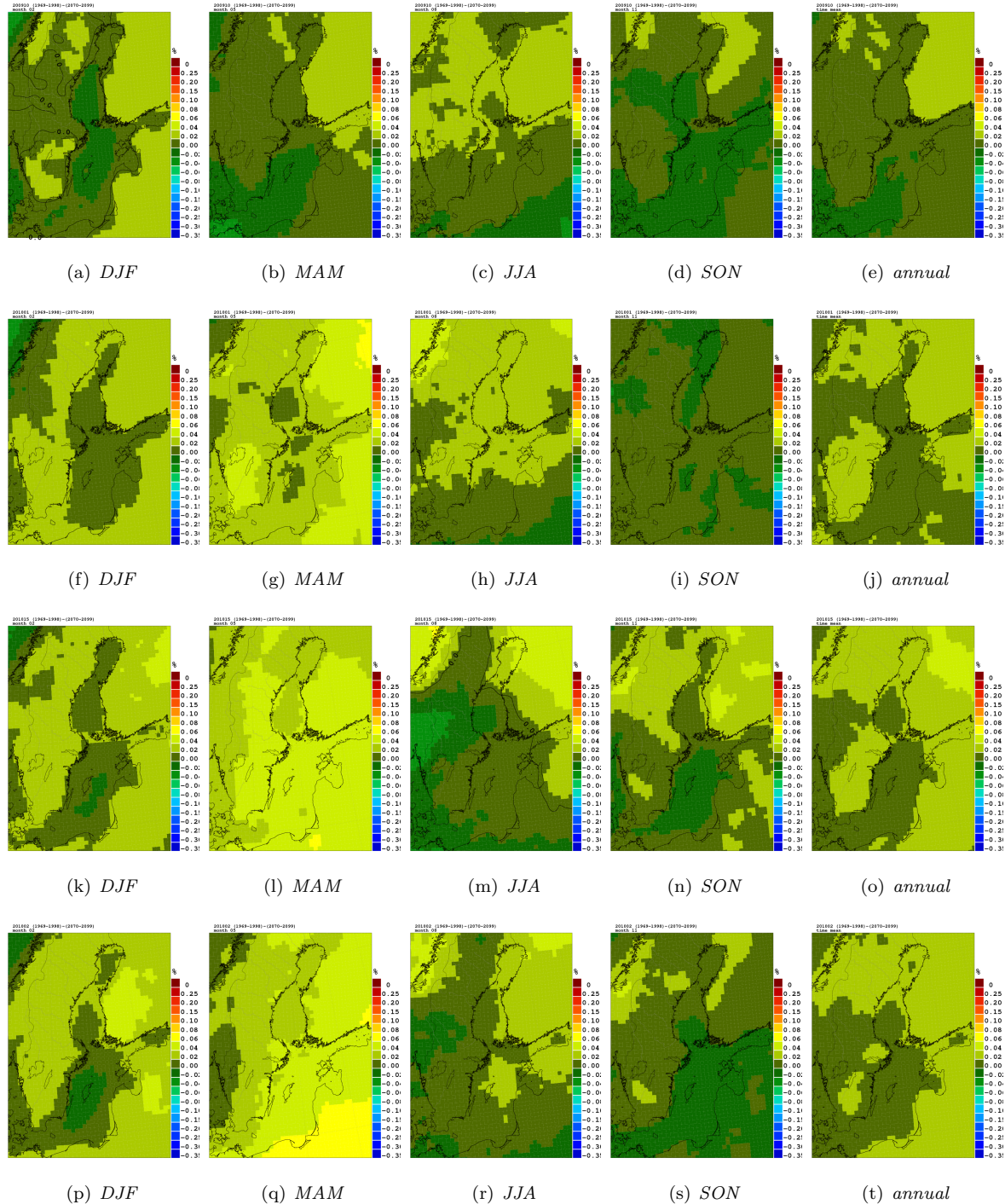


Figure 15. Same as Figure 12 but for cloud cover.

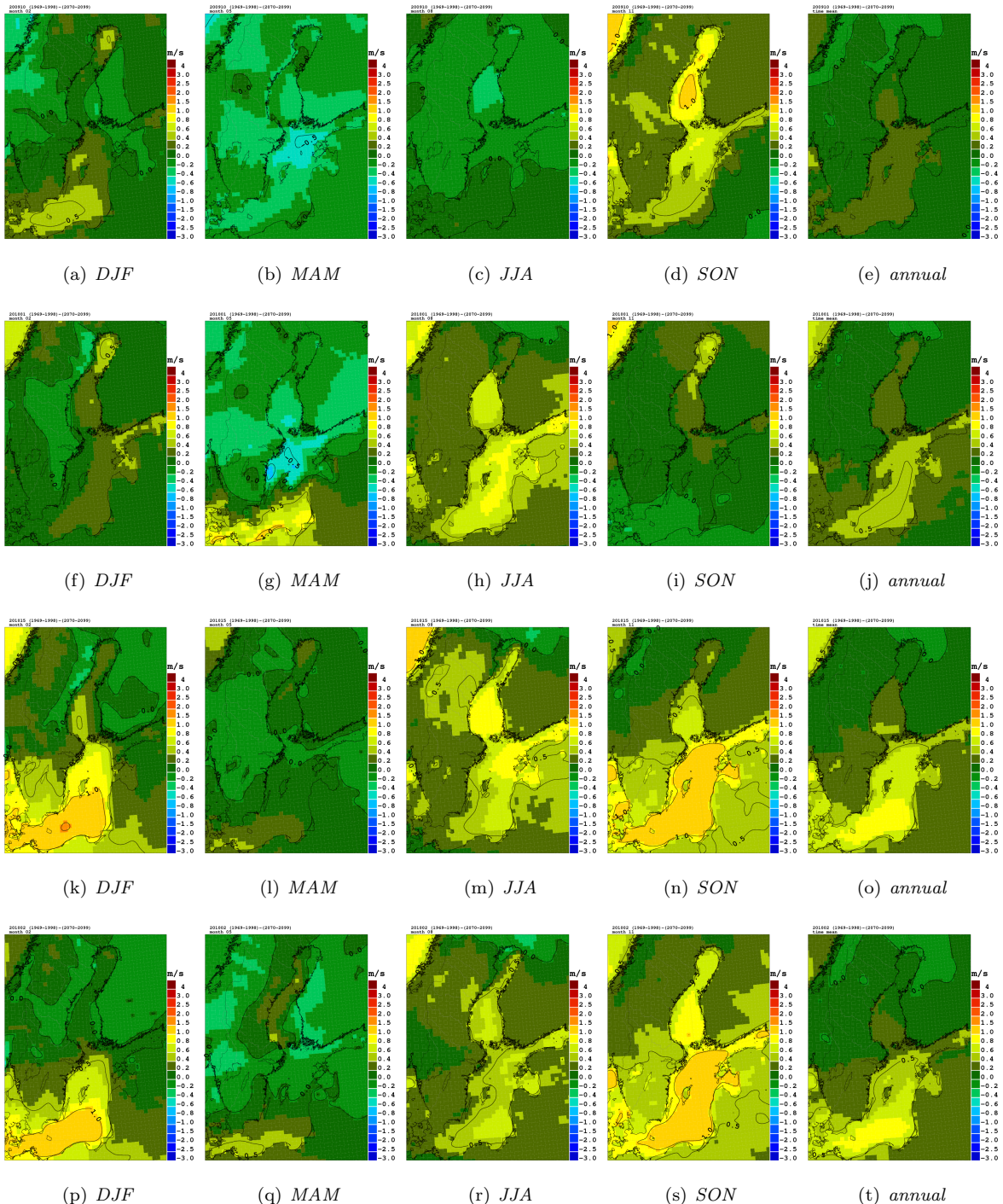


Figure 16. Same as Figure 12 but for 10 m wind speed (in m/s).

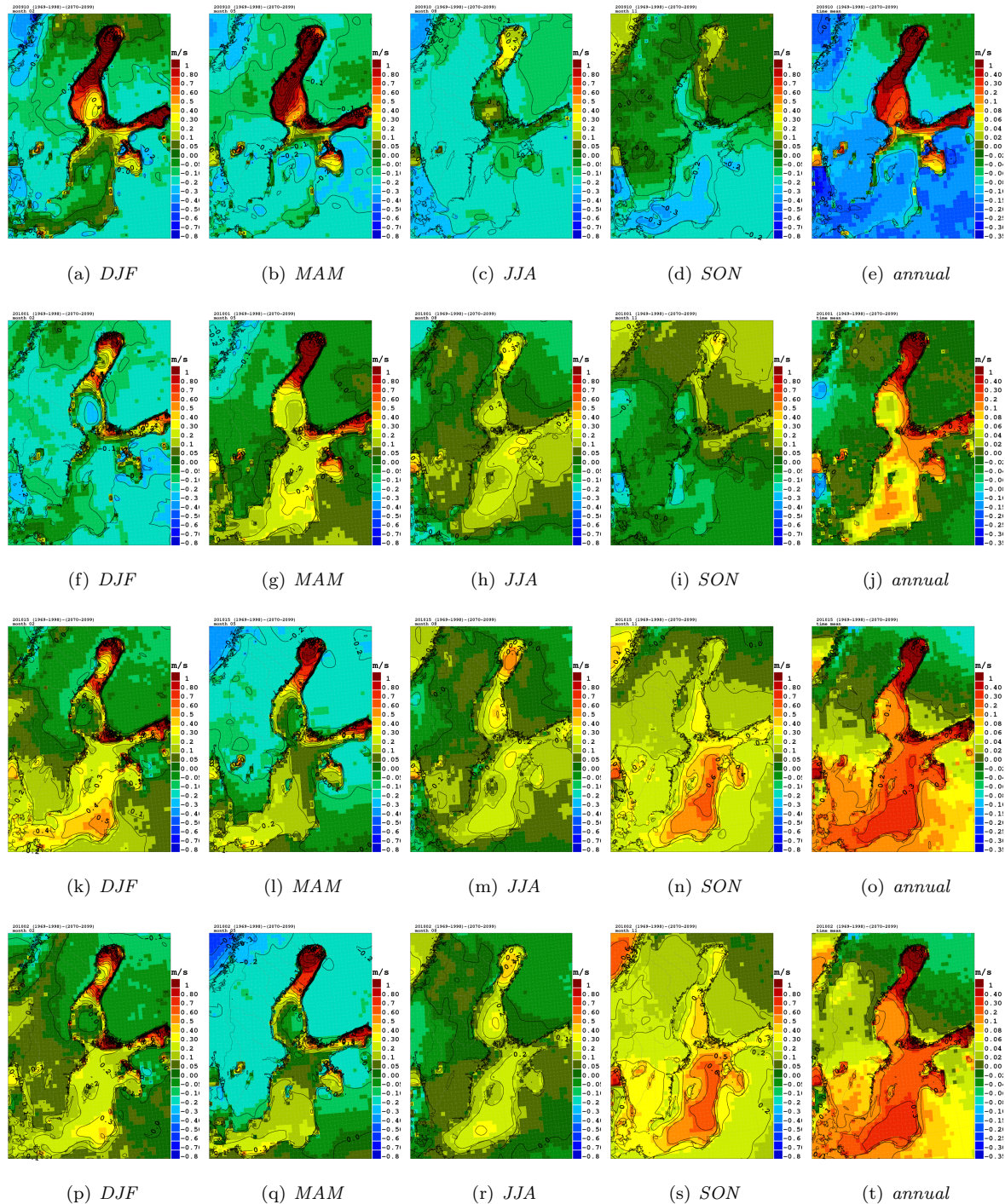


Figure 17. Same as Figure 12 but for the maximum 10 m wind speed (in m/s).

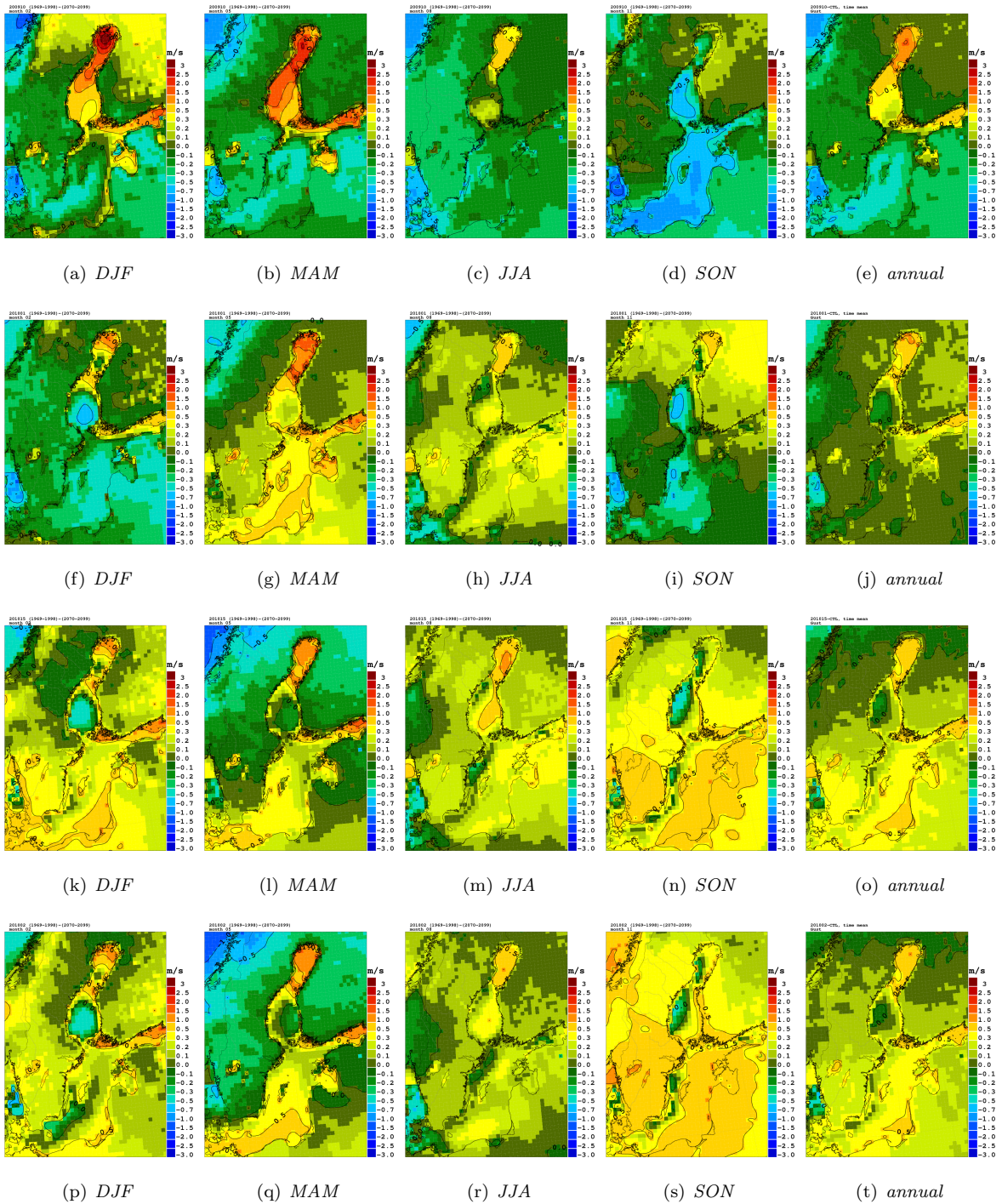


Figure 18. Same as Figure 12 but for the maximum estimated gust wind (in m/s).

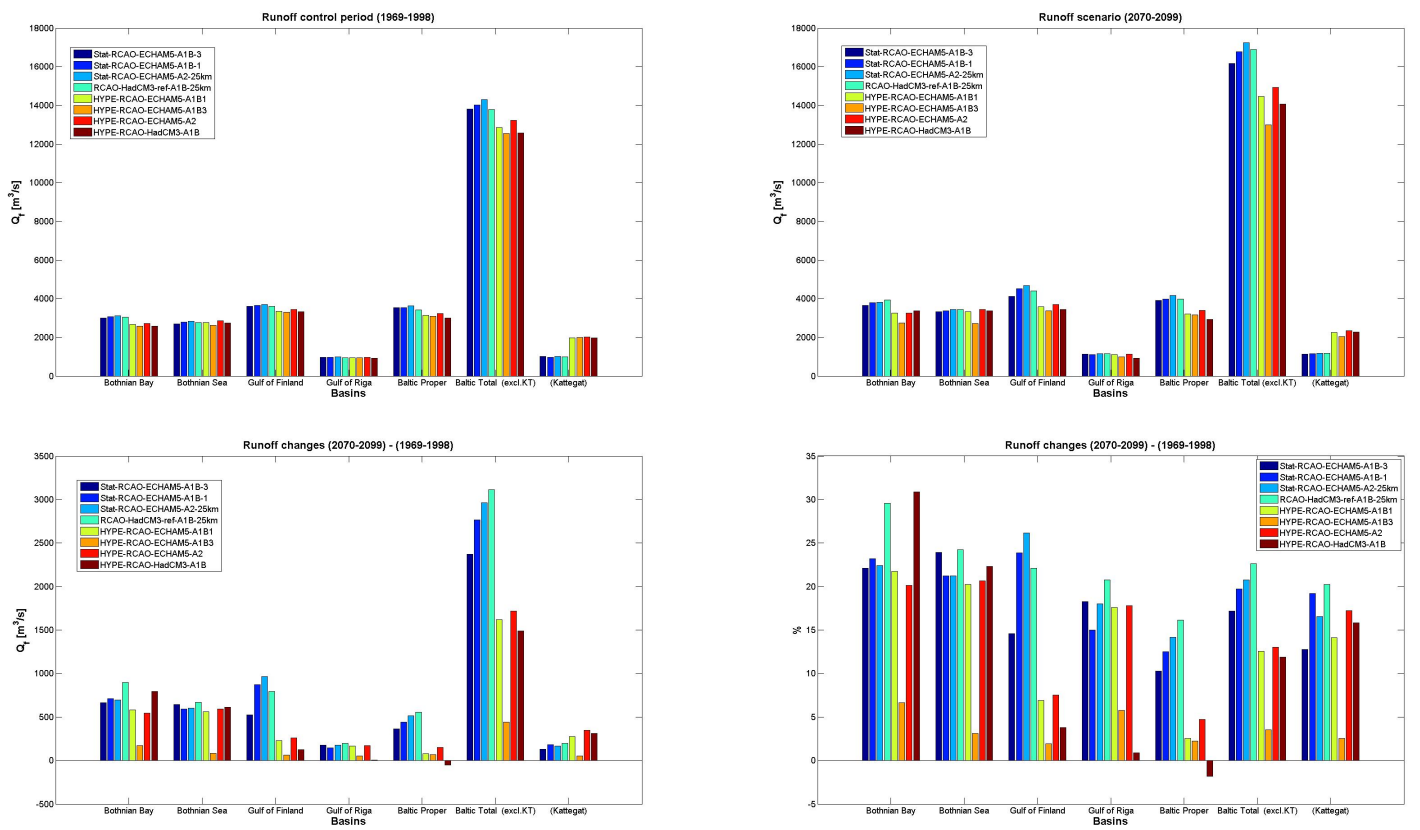


Figure 19. Volume flows (in $m^3 s^{-1}$) in present and future climates calculated with the statistical model (Section 2.3) and with HYPE [Lindström *et al.*, 2010] during the control period 1969-1998 (upper left panel), at the end of the 21st century 2070-2099 (upper right panel) and changes between the periods 2070-2099 and 1969-1998 in absolute (lower left panel) and relative (lower right panel) values. The volume flows into the Bothnian Bay, Bothnian Sea, Gulf of Finland, Gulf of Riga, Baltic proper, total Baltic (without Kattegat) and Kattegat are depicted.